ONLINE SUPPLEMENTAL MATERIALS

CONTENTS

Supplemental Materials and Methods

Supplemental References

Supplemental Figures

- Figure S1: Siglec-6 post-alloHSCT phage panning outputs.
- Figure S2: Fab kinetics for Siglec-6.
- Figure S3: Epitope mapping by HDX-MS/MS.
- Figure S4: Siglec-6 is expressed on primary CLL cells.
- Figure S5: scFv-Fc purification and validation.
- Figure S6: T cell activation markers & cytokines following T-biAb treatment.
- Figure S7: DART-Fc purification and validation.
- Figure S8: RC-1/V9 aDART-Fc efficacy on low expression MEC1-002 cells and at low E:T ratios.
- Figure S9: Targeting Siglec-6 on primary CLL cells.
- Figure S10: CLL-derived T cell expansion and activation.
- Figure S11: Siglec-6 in BTKi-treated CLL patients.
- Figure S12: Siglec-6 T-biAb treatment of healthy donor PBMC.

Supplemental Tables

- Table S1: HDX-MS experimental conditions and data analysis parameters from the guidelines of the IC-HDX-MS community.
- Table S2: CLL patient characteristics.
- Table S3: Representative viability and cell count data from CLL cytotoxicity assays
- Table S4: BTKi-treated CLL patient characteristics.

- Table S5: Healthy donor B cell viability.
- Table S6: Pharmacokinetic parameters of RC-1/V9 aDART-Fc.

Amino Acid Sequences

Cyr MG, *et al. J Immunother Cancer* 2022; 10:e004850. doi: 10.1136/jitc-2022-004850

SUPPLEMENTAL MATERIALS AND METHODS

Cell lines

MEC1 (DSMZ), U937 (ATCC), CII (DSMZ), HG-3 (DSMZ), Jurkat-Lucia NFAT (InvivoGen), FreeStyle 293-F (Thermo Fisher), HEK 293 Phoenix-AMPHO cells (293P, ATCC), HEK293S GnTi$^-$ cells (ATCC), and Expi293F (Thermo Fisher) cell lines were obtained from their respective commercial sources. Cell line MEC1-002 was derived from cell line MEC1 by FACS, as previously reported.[1] The OSU-CLL cell line was provided by Dr. Muthusamy (Ohio State University) under a Material Transfer Agreement (MTA) and Institutional Review Board (IRB) approval.[2] The MDA-BM5 cell line was provided by Dr. Ian McNiece.[3] Firefly luciferase (fLuc)-expressing cells were generated by lentiviral transduction with the epHIV7 vector, as previously described.[4] Transgenic cells stably expressing human Siglec-6 were generated using a hyperactive piggyBac transposase system[5] which was electroporated into CLL cell lines and sorted to generate clonal cell lines. MEC1, MEC1-002, U937, and CII cell lines were cultured in RPMI 1640 supplemented with 10% v/v heat-inactivated fetal bovine serum (hiFBS) (BioFluid Technologies) and 100 U/mL penicillin-streptomycin (pen-strep) and kept at 37°C with 5% CO_2. OSU-CLL cells were cultured similarly but with 20% hiFBS. MDA-BM5 cells were cultured in MEM alpha (Thermo Fisher) with 20% hiFBS and 100 U/mL pen-strep.

Design and cloning of antigens and antibodies

The extracellular domains from human Siglec-6 (accession O43699-1, amino acids (aa) 27-347) and *Macaca mulatta* (rhesus macaque) Siglec-6 (UniProt entry A0A1D5QH63, aa 16-333) were each cloned into pCEP4 at the C-terminus of human IgG1 Fc (aa 99-329). Non-Fc containing Siglec-6 constructs were generated by cloning the V-type and C2-type I Ig-like domains of Siglec-6, aa 28-235 (Siglec-6 VC_{28-235}) from a gene fragment (Twist Bioscience), with a 6xHis tag encoded at the C-terminus, into the pHL-sec vector (Addgene plasmid # 99845) using AgeI

and KpnI restriction sites.[6] *Fabs*. Human Fab-encoding sequences selected by phage display were cloned from pC3C into pET11a, using the restriction enzyme SfiI (New England Biolabs).[7 8] *T-biAbs in scFv-Fc format*. JML-1 scFv and RC-1 scFv gene fragments were synthesized as gBlocks (Integrated DNA Technologies) in the following format: V_H-$(Gly_4\,Ser)_3$ linker-V_L. These scFv fragments were cloned into a pCEP4 vector with an Fc domain containing knob mutations, S354C and T366W previously generated in our lab using KpnI and XhoI restriction enzymes (New England Biolabs). The humanized variant (V9) of the anti-CD3 mAb UCHT1 was incorporated in the Fc-$_{holes}$ arm, as previously described.[9] The anti-CD19 (clone 21D4)/V9 scFv-Fc and anti-HER2 (trastuzumab clone)/V9 scFv-Fc previously reported were used as the positive and negative (non-targeting, NT) controls, respectively.[9 10] *T-biAbs in DART-Fc format*. The Fc component of the DART formats employed gene fragments containing L234A, L235A, P329G mutations to eliminate all Fc-gamma receptor interactions.[11] The knobs-into-holes mutations used in DART-Fc were identical to the scFv-Fc, but the holes-containing half also possessed Fc-star mutations H435Y and R436F to allow for complete heterodimer separation.[12] Symmetric DART (sDART)-Fc constructs were composed of 2 chains, have variable domains each fused to an Fc domain similar to the CDH3 x CD3 DART-Fc PF-06671008, and are named in order that the clones appear on the holes-containing arm.[13] V9/RC-1 sDART-Fc: *$V9_{vk}$-G_3SG_4-$RC\text{-}1_{vh}$-G-CPPCP-Fc-star-$_{holes}$* and *$RC\text{-}1_{vk}$-G_4SG_4-$V9_{vh}$-G-CPPCP-Fc-$_{knobs}$*. RC-1/V9 sDART-Fc: *$RC\text{-}1_{vk}$-G_3SG_4-$V9_{vh}$-G-CPPCP-Fc-star-$_{holes}$* and *$V9_{vk}$-G_4SG_4-$RC\text{-}1_{vh}$-G-CPPCP-Fc-$_{knobs}$*. Asymmetric DART (aDART)-Fc is composed of 3 chains requiring coiled-coil motifs for associating the 2 targeting domains, similar to the CD19 x CD3 DART-Fc duvortuxizumab.[14 15] Chain 1: *$RC\text{-}1_{vk}$-G_3SG_4-$V9_{vh}$ -ASTK-E-coil-G_3-Fc_{knobs};* chain 2: *$V9_{vk}$-G_4SG_4-$RC\text{-}1_{vh}$ -ASTK-K-coil*; chain 3: *Fc_{holes}*. For the negative (non-targeting, NT) aDART-Fc, a human phage-display-derived anti-tetanus toxoid clone TT11[16] was used to replace RC-1. All amino acid sequences can be found at the end of this online supplementary materials file.

Expression and purification of antigens and antibodies

Siglec-6 proteins. Recombinant Fc-siglec fusion proteins for human Siglec-6 and rhesus Siglec-6 were generated in house using FreeStyle 293-F cells and purified via Protein A affinity chromatography.[17] Other siglec-Fc fusions were purchased from R&D Systems. Non-Fc containing Siglec-6 constructs were expressed in HEK293S GnTi$^-$ cells, purified via immobilized metal affinity chromatography (IMAC via HisTrap HP, Cytiva, formerly GE Healthcare Life Sciences).[6 18] For deglycosylation, Siglec-6 glycoprotein at 0.5 mg/mL was subjected to enzymatic treatment using 22,500 U/mL Remove-iT PNGase F (New England Biolabs). After overnight incubation at 37°C, chitin magnetic beads (New England Biolabs) were used to remove the enzyme, and the deglycosylated protein was concentrated for HDX analysis. *Fabs.* Human Fab-encoding sequences selected by phage display were expressed and purified from *E. coli* using IMAC and CaptureSelect Kappa or CH1 resin (both from Thermo Fisher).[7 8] *T-biAbs in scFv-Fc format*. JML-1/V9 and RC-1/V9 scFv-Fc were expressed in 293P cells by co-transfecting the Siglec-6 targeting scFv-Fc-$_{knobs}$ and V9 scFv-Fc-$_{holes}$ pCEP4 plasmids and purified via Protein A affinity chromatography followed by size exclusion chromatography (SEC) with a Superdex 200 increase 10/300 GL column in conjunction with an ÄKTA FPLC instrument (all from Cytiva).[9] *T-biAbs in DART-Fc format*. All DART-Fc constructs were expressed in 293Expi cells (Thermo Fisher) and purified using a 2-step Protein A affinity chromatography process with a MabSelect SuRe (Cytiva) column followed by a POROS MabCapture A (Thermo Fisher) with a pH 6 to pH 3 gradient elution in 50 mM sodium acetate, 500 mM $CaCl_2$ to resolve Fc/Fc-star heterodimers.[19]

Human Fab library selection

The Fab-phage library from a CLL patient who had received an alloHSCT transplant was described previously.[20] The phage were reamplified and selected on plate-coated recombinant human Siglec-6 (Fc-Siglec-6 and Siglec-6-Fc) using established protocols, with minor

adaptations including the use of the ER2378 strain (Lucigen) of *Escherichia coli* for library amplification and 2% non-fat dry milk for blocking.[21 22] Output Fab-phage screening was also conducted according to the established protocols mentioned above.

ELISA

For Fab specificity enzyme-linked immunosorbent assays (ELISAs), 50 ng of each siglec-Fc construct was coated directly into 96-well plates, blocked with 3% BSA, and incubated with 75 ng of the Fab of interest. Binding was detected with peroxidase-conjugated goat anti-human IgG, $F(ab')_2$-specific secondary antibody (Jackson ImmunoResearch) and ABTS One Component HRP Substrate (BioFX). Signal was quantified at 405 nm and 570 nm using a SpectraMax M5 instrument with SoftMax Pro software (Molecular Devices). For cytokine ELISAs, culture supernatants from overnight cytotoxicity assays were diluted and assayed using ELISA MAX Sets (BioLegend) to determine levels of IFN-γ, IL-2, and TNF-α. Cytokine levels were normalized to those of the positive control T-biAb CD19/V9 scFv-Fc at the highest concentration in each experiment.

SPR

Surface plasmon resonance (SPR) studies were carried out on a Biacore X100 instrument (Cytiva, formerly GE Healthcare Life Sciences) as previously described.[4] Fab kinetics were determined by capturing Siglec-6-Fc (5-10 µg/mL) in HBS-EP+ buffer (Cytiva) and injecting titrated Fab. For epitope binning, lower amount of antigen (0.5 µg/mL) was used along with saturating amounts of Fab (10 µM). T-biAb kinetics were determined by capturing Fc-containing T-biAbs and injecting soluble Siglec-6 (aa 28-235-His6) or human CD3ε/δ dimer (ACROBiosystems). Biacore evaluation software was used to calculate k_{on}, k_{off}, and K_d.

Homology modeling of Siglec-6

A homology model of Siglec-6 (aa 27-236) was generated using Phyre2,[23] and CD33 (71% identity), the most similar protein with a published structure, was selected as the template for modeling. PROCHECK was employed to assess model quality,[24] and automated optimization was performed using YASARA.[25]

Hydrogen-deuterium exchange (HDX) detected by mass spectrometry (MS)

Solution-phase amide HDX experiments were carried out with a fully automated system (CTC HTS PAL, LEAP Technologies, Carrboro, NC; housed inside a 4°C cabinet) as described[26] with slight modifications. Peptides were identified using tandem MS (MS/MS) experiments performed on a QExactive (Thermo Fisher) over a 70 min gradient. Product ion spectra were acquired in a data-dependent mode and the five most abundant ions were selected for the product ion analysis per scan event. The MS/MS *.raw data files were converted to *.mgf files and then submitted to MASCOT (version 2.3 Matrix Science, London, UK) for peptide identification. The maximum number of missed cleavages was set at 4 with the mass tolerance for precursor ions ± 0.6 Da and for fragment ions ± 8ppm. Oxidation to methionine was selected for variable modification. Pepsin was used for digestion and no specific enzyme was selected in MASCOT during the search. Peptides included in the peptide set used for HDX detection had a MASCOT score of 20 or greater. The MS/MS MASCOT search was also performed against a decoy (reverse) sequence and false positives were ruled out if they did not pass a 1% false discovery rate.

10 µM Siglec-6 was preincubated with RC-1 Fab at a 1:1 molar ratio for 1 h on ice for complex formation before subjecting them to HDX analysis. For the differential HDX experiments, 5 µL either Siglec-6 (Apo) or the complex (1:1 molar mixture Siglec-6 and RC-1 Fab) were mixed with 20 µL of D_2O-containing HDX buffer (10 mM sodium phosphate, 150 mM NaCl, pH 7.8) and incubated at 4°C for 0, 10, 30, 60, 900 or 3,600 s. Following on-exchange, unwanted forward- or back-exchange was minimized, and the protein was denatured by the

addition of 25 µL of a quench solution (3 M urea, 1% TFA, pH 2.5). Samples were then immediately passed through an immobilized pepsin column (2 mm x 2 cm, prepared in house) at 200 µL min^{-1} (0.1% v/v TFA, 4°C) and the resulting peptides were trapped and desalted on a 2 mm × 10 mm C_8 trap column (Hypersil Gold, Thermo Fisher). The bound peptides were then gradient-eluted (4-40% CH_3CN v/v and 0.3% v/v formic acid) across a 2.1 mm × 50 mm C_{18} separation column (Hypersil Gold, Thermo Fisher) for 5 min. Sample handling and peptide separation were conducted at 4°C. The eluted peptides were then subjected to electrospray ionization directly coupled to a high resolution Orbitrap mass spectrometer (Exactive, Thermo Fisher).

The differential HDX experiment was performed with three technical replicates. The intensity weighted mean m/z centroid value of each peptide envelope was calculated and subsequently converted into a percentage of deuterium incorporation. This is accomplished by determining the observed averages of the undeuterated and fully deuterated spectra using the conventional formula described elsewhere.[27] The fully deuterated control, 100% deuterium incorporation, was calculated theoretically, and corrections for back-exchange were made based on an estimated 70% deuterium recovery and accounting for 80% final deuterium concentration in the sample (1:5 dilution in D_2O HDX buffer). Statistical significance for the differential HDX data is determined by an unpaired t-test for each time point, a procedure that is integrated into the HDX Workbench software.[28]

The HDX data from all overlapping peptides were consolidated to individual amino acid values using a residue averaging approach. Briefly, for each residue, the deuterium incorporation values and peptide lengths from all overlapping peptides were assembled. A weighting function was applied in which shorter peptides were weighted more heavily and longer peptides were weighted less. Each of the weighted deuterium incorporation values were then averaged incorporating this weighting function to produce a single value for each amino

acid. The initial two residues of each peptide, as well as prolines, were omitted from the calculations. This approach is similar to that previously described.[29]

Deuterium uptake for each peptide is calculated as the average of % D for all on-exchange time points and the difference in average %D values between the unbound and bound samples is presented as a heat map with a color code given at the bottom of the figure (warm colors for deprotection and cool colors for protection). Peptides are colored by the software automatically to display significant differences, determined either by a >5% difference (less or more protection) in average deuterium uptake between the two states, or by using the results of unpaired t-tests at each time point (p-value < 0.05 for any two time points or a p-value < 0.01 for any single time point). Peptides with non-significant changes between the two states are colored grey. The exchange at the first two residues for any given peptide is not colored. Each peptide bar in the heat map view displays the average Δ %D values, associated standard deviation, and the charge state. Additionally, overlapping peptides with a similar protection trend covering the same region are used to rule out data ambiguity.

The data have been deposited to the ProteomeXchange Consortium via the PRIDE[30] partner repository with the data set identifier PXD029601.

Flow cytometry

Fabs were used to stain cells at a concentration of 2 µg/mL, unless otherwise noted. Biotinylated antibody binding was detected using Alexa Fluor 647-streptavidin (Jackson ImmunoResearch) or PE-streptavidin (BD Biosciences). T-biAb was used between 0.1 and 10 µg/mL and detected using an Alexa Fluor 647-goat anti-human IgG1-Fc specific polyclonal antibody (Jackson ImmunoResearch). Commercial mAbs used for flow cytometry targeting Siglec-6 (R&D Systems, 767329), CD5 (BioLegend, L17F12), CD20 (BD Biosciences, L27), CD3 (BioLegend, OKT3), CD4 (BD, RPA-T4), CD8 (BD Biosciences, HIT8a), CD69 (BioLegend, FN50), and CD25 (BioLegend, BC96) were purchased and used at the recommended dilutions.

Samples were analyzed on either an Accuri C6 Plus or a LSRII flow cytometer (both from BD Biosciences)

PK study

Six- to seven-week-old female NOD-*scid* IL2Rγ^{null} (NSG) mice (JAX #005557) were pre-conditioned with 0.25 mL human serum or DPBS one day prior to treatment. Three to four mice per group were injected i.v. or i.p. with RC-1/V9 aDART-Fc at 2.5 mg/kg. Blood was collected at 5 min, 30 min, 2, 8, 24, 48, 72, 96, 144, 216, 336, and 528 h after injection, maintaining treatment order with blood collection, into heparinized capillary tubes from the tail vein. Plasma was obtained by centrifuging the samples at 2,000 × g for 5 min and was stored at −80°C until analysis. The concentration of T-biAbs in the plasma samples was measured by ELISA. CD3ε/δ (ACROBiosystems) was coated directly onto half-area ELISA plates (200 ng/well) overnight and blocked with 3% w/v bovine serum albumin (BSA). Serum samples or T-biAb standard were added to the plate followed by 2-h incubation, and T-biAb was detected with HRP-conjugated AffiniPure goat anti-human-Fc secondary antibody (Jackson ImmunoResearch). The concentration of T-biAb in the plasma samples was interpolated from a four-parameter logistic model fit of the standard curve (GraphPad Prism). PK parameters were calculated from the time points within the linear range by using Phoenix WinNonlin PK/PD Modeling and Analysis software (Pharsight).

Statistics

Statistical significance for the differential HDX data is determined by an unpaired t-test for each time point, a procedure that is integrated into the HDX Workbench software.[28] For biochemical and *in vitro* data, a two-tailed student's t-test was used to determine calculate statistics. To compare the effects of multiple *ex vivo* treatments on each patient sample, Wilcoxon matched-pairs signed rank test was used. For *in vivo* studies, 4 (PK study) to 5 (treatment model) mice

were randomized and treated per experimental group, based on the resource equation method, as there were multiple readouts.[31] Treatment and analysis were unblinded. Welch's t-test was used to compare bioluminescent signal among treatment groups, as standard deviation was not uniform across groups, while the Mantel-Cox log-rank analysis was used to compare survival advantages. Statistical analysis was conducted using GraphPad Prism and significance was established if $p < 0.05$, unless otherwise noted.

SUPPLEMENTAL REFERENCES

1. Chang J, Peng H, Shaffer BC, et al. Siglec-6 on Chronic Lymphocytic Leukemia Cells Is a Target for Post-Allogeneic Hematopoietic Stem Cell Transplantation Antibodies. *Cancer Immunol Res* 2018;6(9):1008-13. doi: 10.1158/2326-6066.Cir-18-0102 [published Online First: 2018/07/08]
2. Hertlein E, Beckwith KA, Lozanski G, et al. Characterization of a new chronic lymphocytic leukemia cell line for mechanistic in vitro and in vivo studies relevant to disease. *PLoS One* 2013;8(10):e76607. doi: 10.1371/journal.pone.0076607 [published Online First: 2013/10/17]
3. Kellner J, Wierda W, Shpall E, et al. Isolation of a novel chronic lymphocytic leukemic (CLL) cell line and development of an in vivo mouse model of CLL. *Leuk Res* 2016;40:54-9. doi: 10.1016/j.leukres.2015.10.008 [published Online First: 2015/11/26]
4. Peng H, Nerreter T, Chang J, et al. Mining Naive Rabbit Antibody Repertoires by Phage Display for Monoclonal Antibodies of Therapeutic Utility. *J Mol Biol* 2017;429(19):2954-73. doi: 10.1016/j.jmb.2017.08.003 [published Online First: 2017/08/19]
5. Yusa K, Zhou L, Li MA, et al. A hyperactive piggyBac transposase for mammalian applications. *Proc Natl Acad Sci U S A* 2011;108(4):1531-6. doi: 10.1073/pnas.1008322108 [published Online First: 2011/01/06]
6. Aricescu AR, Lu W, Jones EY. A time- and cost-efficient system for high-level protein production in mammalian cells. *Acta Crystallogr D Biol Crystallogr* 2006;62(Pt 10):1243-50. doi: 10.1107/S0907444906029799 [published Online First: 2006/09/27]
7. Kwong KY, Rader C. E. coli expression and purification of Fab antibody fragments. *Curr Protoc Protein Sci* 2009;Chapter 6:Unit 6 10. doi: 10.1002/0471140864.ps0610s55 [published Online First: 2009/02/24]
8. Stahl SJ, Watts NR, Rader C, et al. Generation and characterization of a chimeric rabbit/human Fab for co-crystallization of HIV-1 Rev. *J Mol Biol* 2010;397(3):697-708. doi: 10.1016/j.jmb.2010.01.061 [published Online First: 2010/02/09]
9. Qi J, Li X, Peng H, et al. Potent and selective antitumor activity of a T cell-engaging bispecific antibody targeting a membrane-proximal epitope of ROR1. *Proc Natl Acad Sci U S A* 2018;115(24):E5467-e76. doi: 10.1073/pnas.1719905115 [published Online First: 2018/05/31]
10. Robinson HR, Qi J, Cook EM, et al. A CD19/CD3 bispecific antibody for effective immunotherapy of chronic lymphocytic leukemia in the ibrutinib era. *Blood* 2018;132(5):521-32. doi: 10.1182/blood-2018-02-830992 [published Online First: 2018/05/11]
11. Schlothauer T, Herter S, Koller CF, et al. Novel human IgG1 and IgG4 Fc-engineered antibodies with completely abolished immune effector functions. *Protein Eng Des Sel* 2016;29(10):457-66. doi: 10.1093/protein/gzw040 [published Online First: 2016/09/01]
12. Jendeberg L, Nilsson P, Larsson A, et al. Engineering of Fc(1) and Fc(3) from human immunoglobulin G to analyse subclass specificity for staphylococcal protein A. *J Immunol Methods* 1997;201(1):25-34. doi: 10.1016/s0022-1759(96)00215-3 [published Online First: 1997/02/14]
13. Root AR, Cao W, Li B, et al. Development of PF-06671008, a Highly Potent Anti-P-cadherin/Anti-CD3 Bispecific DART Molecule with Extended Half-Life for the Treatment of Cancer. *Antibodies (Basel)* 2016;5(1) doi: 10.3390/antib5010006 [published Online First: 2016/03/04]
14. Liu L, Lam CK, Long V, et al. MGD011, A CD19 x CD3 Dual-Affinity Retargeting Bi-specific Molecule Incorporating Extended Circulating Half-life for the Treatment of B-Cell

Malignancies. *Clin Cancer Res* 2017;23(6):1506-18. doi: 10.1158/1078-0432.Ccr-16-0666 [published Online First: 2016/09/25]
15. World Health Organization, Drug Information 2016, vol. 30, 4 *WHO Drug Information* 2016;30(4):545-604.
16. Kwong KY, Baskar S, Zhang H, et al. Generation, affinity maturation, and characterization of a human anti-human NKG2D monoclonal antibody with dual antagonistic and agonistic activity. *J Mol Biol* 2008;384(5):1143-56. doi: 10.1016/j.jmb.2008.09.008 [published Online First: 2008/09/24]
17. Kovalovsky D, Yoon JH, Cyr MG, et al. Siglec-6 is a target for chimeric antigen receptor T-cell treatment of chronic lymphocytic leukemia. *Leukemia* 2021;35:2581–91. doi: 10.1038/s41375-021-01188-3
18. Ereño-Orbea J, Sicard T, Cui H, et al. Characterization of Glycoproteins with the Immunoglobulin Fold by X-Ray Crystallography and Biophysical Techniques. *J Vis Exp* 2018;137:57750. doi: 10.3791/57750 [published Online First: 2018/07/24]
19. Tustian AD, Endicott C, Adams B, et al. Development of purification processes for fully human bispecific antibodies based upon modification of protein A binding avidity. *mAbs* 2016;8(4):828-38. doi: 10.1080/19420862.2016.1160192 [published Online First: 2016/03/11]
20. Baskar S, Suschak JM, Samija I, et al. A human monoclonal antibody drug and target discovery platform for B-cell chronic lymphocytic leukemia based on allogeneic hematopoietic stem cell transplantation and phage display. *Blood* 2009;114(20):4494-502. doi: 10.1182/blood-2009-05-222786 [published Online First: 2009/08/12]
21. Rader C. Generation of human Fab libraries for phage display. *Methods Mol Biol* 2012;901:53-79. doi: 10.1007/978-1-61779-931-0_4 [published Online First: 2012/06/23]
22. Rader C. Selection of human Fab libraries by phage display. *Methods Mol Biol* 2012;901:81-99. doi: 10.1007/978-1-61779-931-0_5 [published Online First: 2012/06/23]
23. Kelley LA, Mezulis S, Yates CM, et al. The Phyre2 web portal for protein modeling, prediction and analysis. *Nature Protocols* 2015;10(6):845-58. doi: 10.1038/nprot.2015.053
24. Laskowski RA, MacArthur MW, Moss DS, et al. PROCHECK: a program to check the stereochemical quality of protein structures. *J Appl Crystallogr* 1993;26(2):283-91. doi: https://doi.org/10.1107/S0021889892009944
25. Krieger E, Vriend G. New ways to boost molecular dynamics simulations. *J Comput Chem* 2015;36(13):996-1007. doi: 10.1002/jcc.23899 [published Online First: 2015/04/01]
26. Chalmers MJ, Busby SA, Pascal BD, et al. Probing protein ligand interactions by automated hydrogen/deuterium exchange mass spectrometry. *Anal Chem* 2006;78(4):1005-14. doi: 10.1021/ac051294f [published Online First: 2006/02/16]
27. Zhang Z, Smith DL. Determination of amide hydrogen exchange by mass spectrometry: a new tool for protein structure elucidation. *Protein Sci* 1993;2(4):522-31. doi: 10.1002/pro.5560020404 [published Online First: 1993/04/01]
28. Pascal BD, Willis S, Lauer JL, et al. HDX workbench: software for the analysis of H/D exchange MS data. *J Am Soc Mass Spectrom* 2012;23(9):1512-21. doi: 10.1007/s13361-012-0419-6 [published Online First: 2012/06/14]
29. Keppel TR, Weis DD. Mapping residual structure in intrinsically disordered proteins at residue resolution using millisecond hydrogen/deuterium exchange and residue averaging. *J Am Soc Mass Spectrom* 2015;26(4):547-54. doi: 10.1007/s13361-014-1033-6 [published Online First: 2014/12/08]
30. Perez-Riverol Y, Csordas A, Bai J, et al. The PRIDE database and related tools and resources in 2019: improving support for quantification data. *Nucleic Acids Res* 2019;47(D1):D442-D50. doi: 10.1093/nar/gky1106 [published Online First: 2018/11/06]

31. Charan J, Kantharia ND. How to calculate sample size in animal studies? *J Pharmacol Pharmacother* 2013;4(4):303-6. doi: 10.4103/0976-500x.119726 [published Online First: 2013/11/20]

SUPPLEMENTAL FIGURES

Antigen	Siglec-6 Fc (C-term)				Fc-Siglec-6 (N-term)			
Round	1	2	3	4	1	2	3	4
Enrichment		0.00	7.96	1.14		0.01	0.06	475

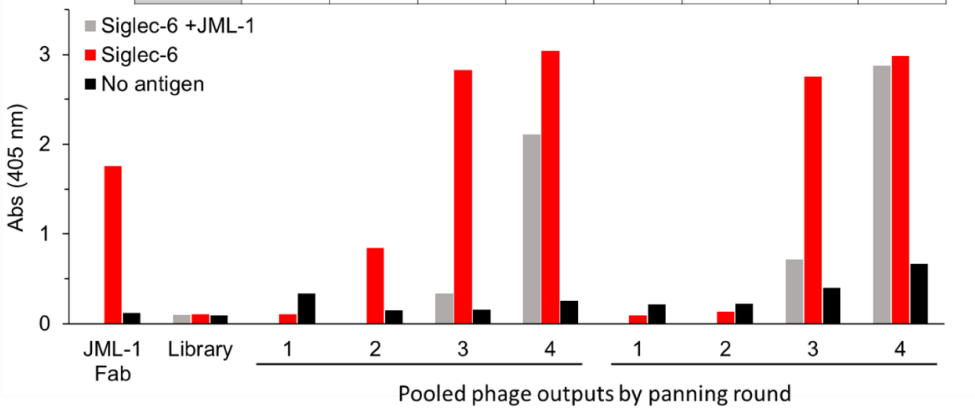

Figure S1: Siglec-6 post-alloHSCT phage panning outputs. Enrichment was observed in the phage output titer through subsequent panning rounds (top). Fab-phage ELISA data (bottom) demonstrating that both panning experiments generated polyclonal phage that bind to Siglec-6 in the presence or absence of JML-1 Fab. Abs = absorbance.

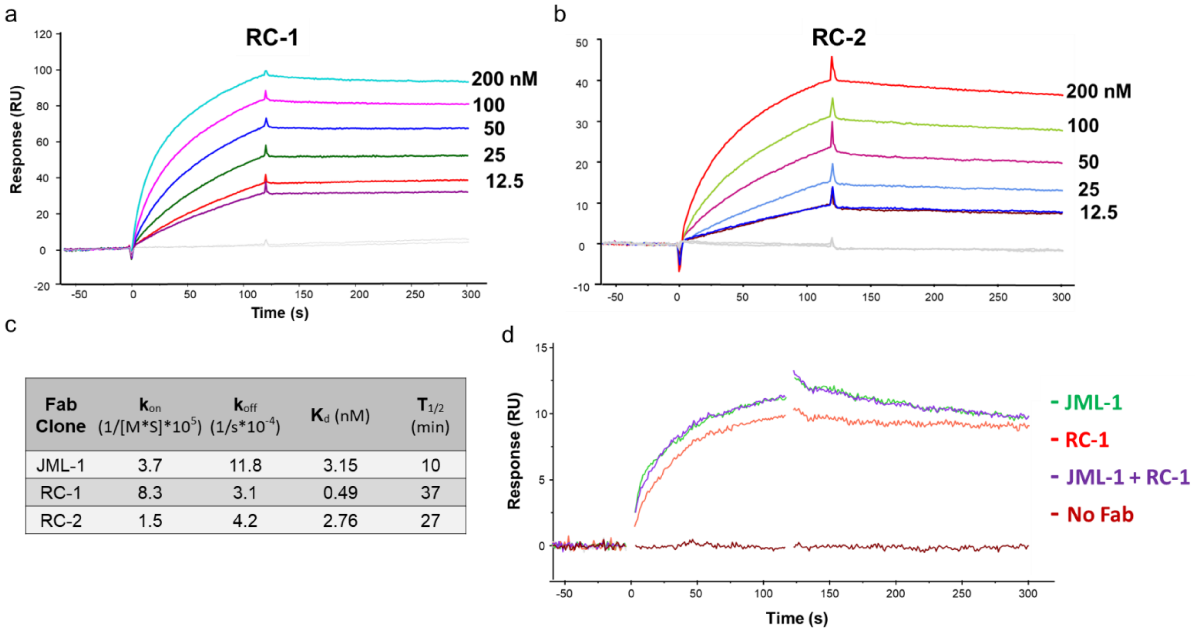

Fab Clone	k_{on} ($1/[M*S]*10^5$)	k_{off} ($1/s*10^{-4}$)	K_d (nM)	$T_{1/2}$ (min)
JML-1	3.7	11.8	3.15	10
RC-1	8.3	3.1	0.49	37
RC-2	1.5	4.2	2.76	27

Figure S2: Fab kinetics for Siglec-6. SPR sensorgrams of soluble Fabs RC-1 (a) and RC-2 (b) binding to Fc-Siglec-6 (5 µg/mL). (c) Table of SPR data (d) SPR sensorgram demonstrating that there is no additive effect of RC-1 over JML-1 alone (1 µM each, saturating) validating that the two antibody clones target overlapping epitopes and cannot bind simultaneously to Fc-Siglec-6 (0.5 µg/mL).

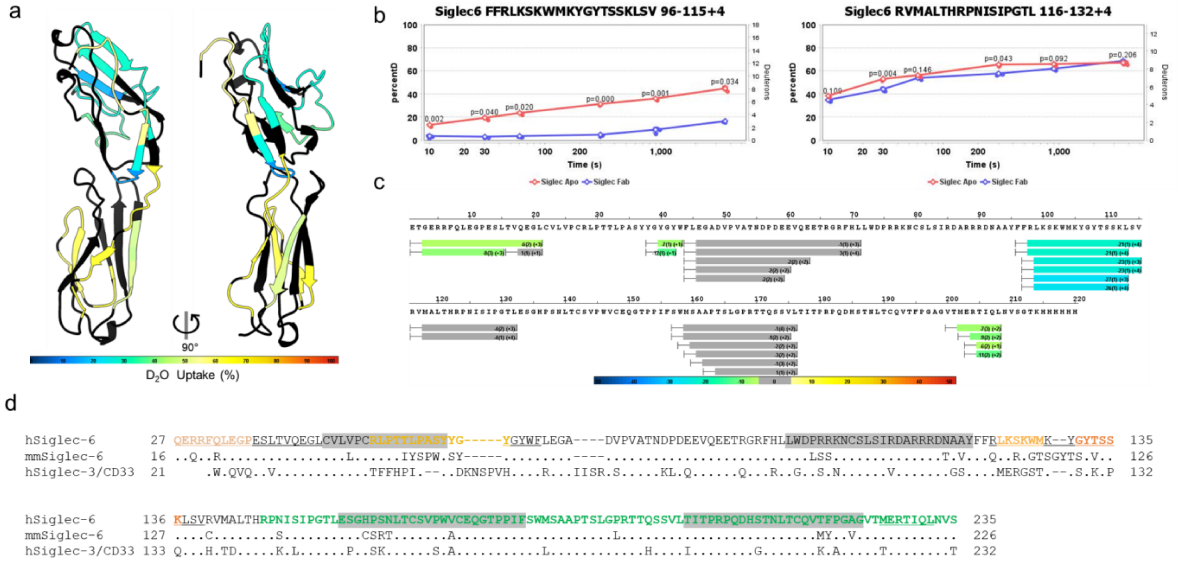

Figure S3: Epitope mapping by HDX-MS. (a) Homology model (see Supplemental Materials and Methods) of the two N-terminal Siglec-6 V and C2i domains overlayed with colors to indicate the level of deuterium uptake of the ectodomain fragment in the absence of Fab. (b) Deuterium uptake versus time plots for two selected peptides, with the results from the Siglec-6 ectodomain fragment alone (red) and its complex with RC-1 Fab (blue). These plots are representative of peptides that show reduced (left) or unchanged (right) uptake in the presence of Fab. (c) Sequence map of the Siglec-6 construct used for HDX-MS (note: the N- and C-terminal expression tags differ from the WT sequence, see Supplemental Materials and Methods) with coloring corresponding to the differential deuterium uptake data +/- Fab. (d) Sequence alignment of human Siglec-6 (V and C2i domains, 27-235), rhesus macaque Siglec-6 (UniProt accession A0A1D5QH63, 16-226) and human CD33 (21-232), with dots indicating identity to Siglec-6. The underlined residues were part of peptides that showed differential deuterium uptake in the presence of Fab. The grey highlighted regions indicate that the peptides were not observed in the MS data. Residues colored in shades of yellow and orange (matches **Fig. 1e, f**) are required for Fab binding in ELISA, while green indicates regions that are not required for binding in ELISA. The numbering shown in this alignment is based on full-length, canonical isoforms found in the UniProtKB database.

a

	CLL Patient ID	Siglec-6 (ABC-Isotype)
	2691	6,035
	4973	3,671
	11944	3,585
	4705	2,431
	3071	1,536
	8242	843

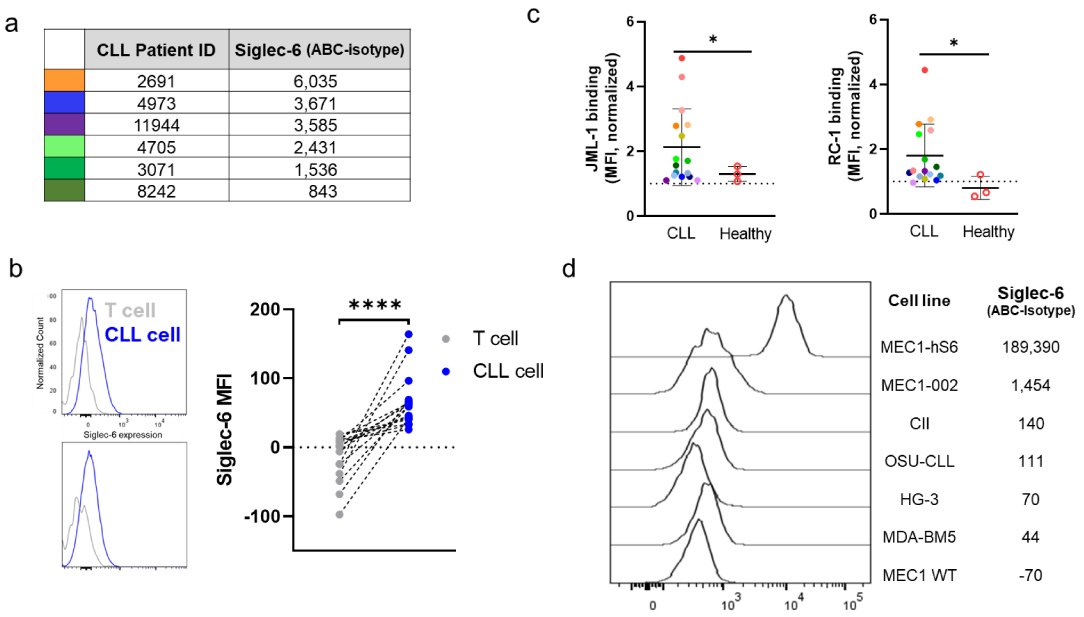

Figure S4: Siglec-6 is expressed on primary CLL cells. (a) Quantification of Siglec-6 expression (mouse mAb 767329) on primary CLL cells (live, CD20$^+$ CD5$^+$, n=6) with color coding to identify each sample. ABC denotes antibody binding capacity = 1 to 2 copies of the receptor on the cell surface per antibody bound. (b) Flow cytometry staining of primary CLL cells using mouse mAb 767329. Representative histograms (left) and quantified mean fluorescence intensity (MFI, right) demonstrate Siglec-6 is expressed on CLL cells (live, CD20$^+$ CD5$^+$ shown in blue) yet absent on T cells (CD3$^+$ CD5$^+$, grey) from individual CLL patients (n=16). Statistics were calculated using Wilcoxon matched-pairs signed rank test **** p<0.0001. (c) Binding of human anti-Siglec-6 clone JML-1 (biotinylated IgG1, left) or RC-1 (biotinylated Fab) to CLL and healthy donor PBMC. Each point represents an individual patient. Since staining was done on different days, the data in each experiment were normalized to staining with an isotype control antibody for each patient and the dotted line marks the level of isotype binding. Statistics were calculated using an unpaired t test with Welch's correction, * p<0.05. (d) Quantification of Siglec-6 levels on CLL-derived cell lines as ABC using mouse mAb 767329 or isotype control and a bead calibration standard. MEC1-hS6 refers to a clone of MEC1 that had been stably transfected to overexpress Siglec-6.

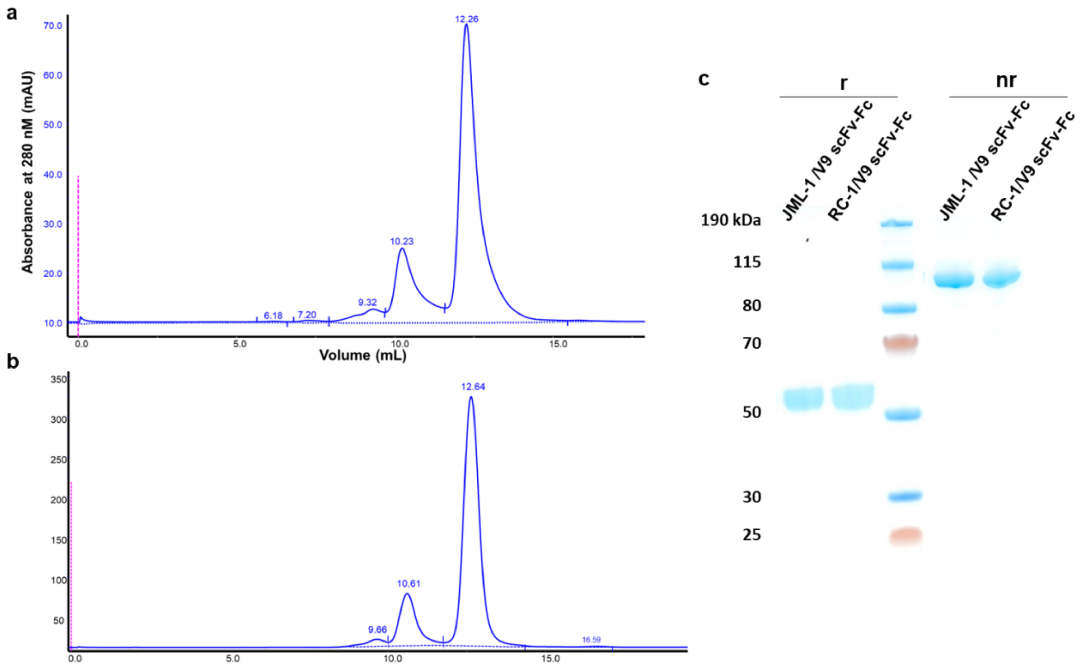

Figure S5: scFv-Fc purification and validation. After an initial round of Protein A affinity chromatography purification, size exclusion chromatography (SEC) was used to purify JML-1/V9 scFv-Fc (a) and RC-1/V9 scFv-Fc (b). The resulting chromatograms are shown and the major 105 kDa peak occurring around 12 mL for each, was isolated and verified to be free of aggregates by reducing (r) and non-reducing (nr) SDS-PAGE and Coomassie Blue staining (c).

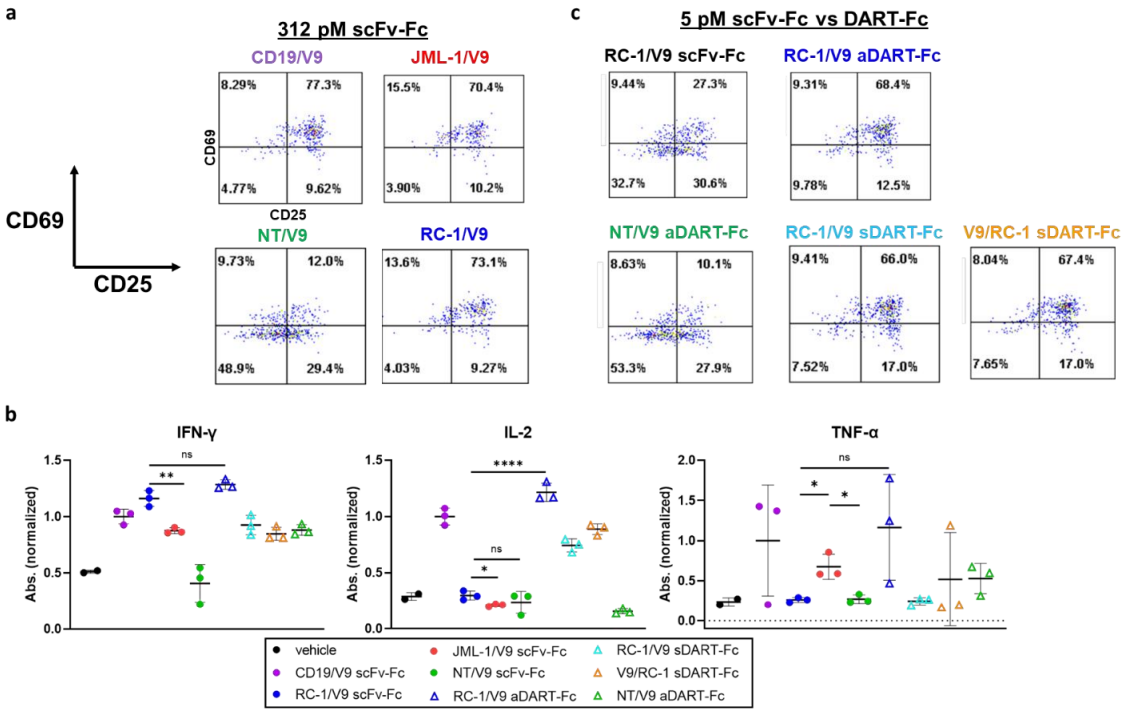

Figure S6: T cell activation markers & cytokines following T-biAb treatment. (a) MEC1-hS6 cells were co-cultured with human T cells at a 1:1 E:T ratio and a titration of the indicated T-biAbs. Following overnight incubation, T cells were stained for activation markers CD69 and CD25. Shown are representative scatterplots from cells treated with 312 pM scFv-Fc (a) and 5 pM of scFv-Fc or DART-Fc (c). (b) MEC1-002 ($hS6^{lo}$) cells were cultured overnight with T cells at a 1:1 E:T ratio in the presence of 800 pM of T-biAb, and the levels of type I cytokines in the co-culture supernatants were determined by ELISA.

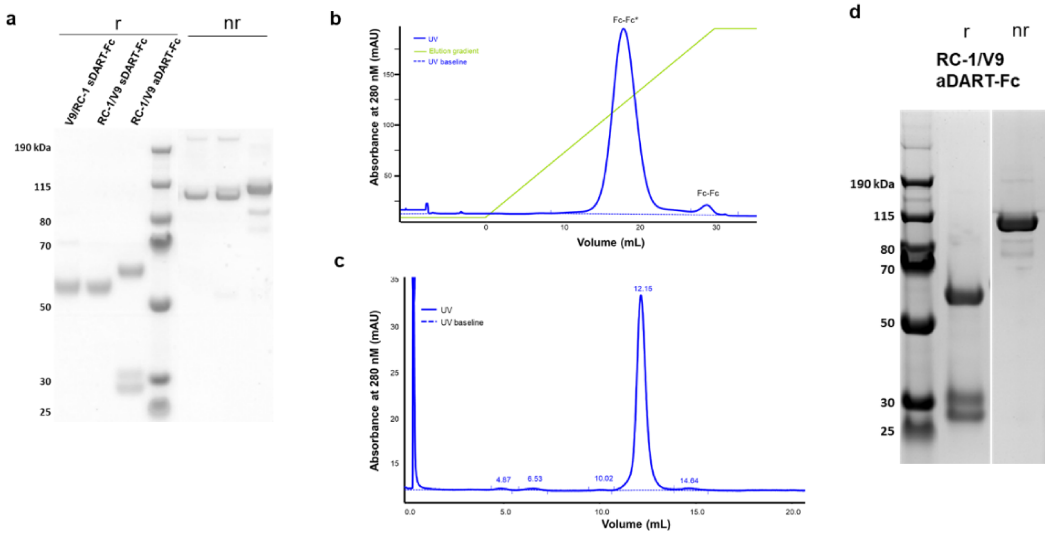

Figure S7: DART-Fc purification and validation. (a) Reducing (r) and non-reducing (nr) Coomassie Blue-stained SDS-PAGE gel of DARTs after an initial round of MabSelect SuRe Protein A affinity chromatography purification revealed the expected size of the monomers in the non-reducing lanes and the dimer (sDART-Fc) or trimer (aDART-Fc) in the reducing lanes. (b) To eliminate the lower molecular weight bands observed in the RC-1/V9 aDART-Fc, selective heterodimer purification was conducted by gradient elution from the POROS mAb Capture A column which allows for separation of Fc-Fc* heterodimers and Fc-Fc homodimers on the basis of differential affinities in the presence of 500 mM calcium chloride, a chaotropic salt. (c) Analytical SEC area under the curve (AUC) analysis revealed >96% of the protein in the major peak corresponding to the 107.9 kDa RC-1/V9 aDART-Fc trimer. (d) SDS-PAGE verified the improved purity of the final RC-1/V9 aDART-Fc product.

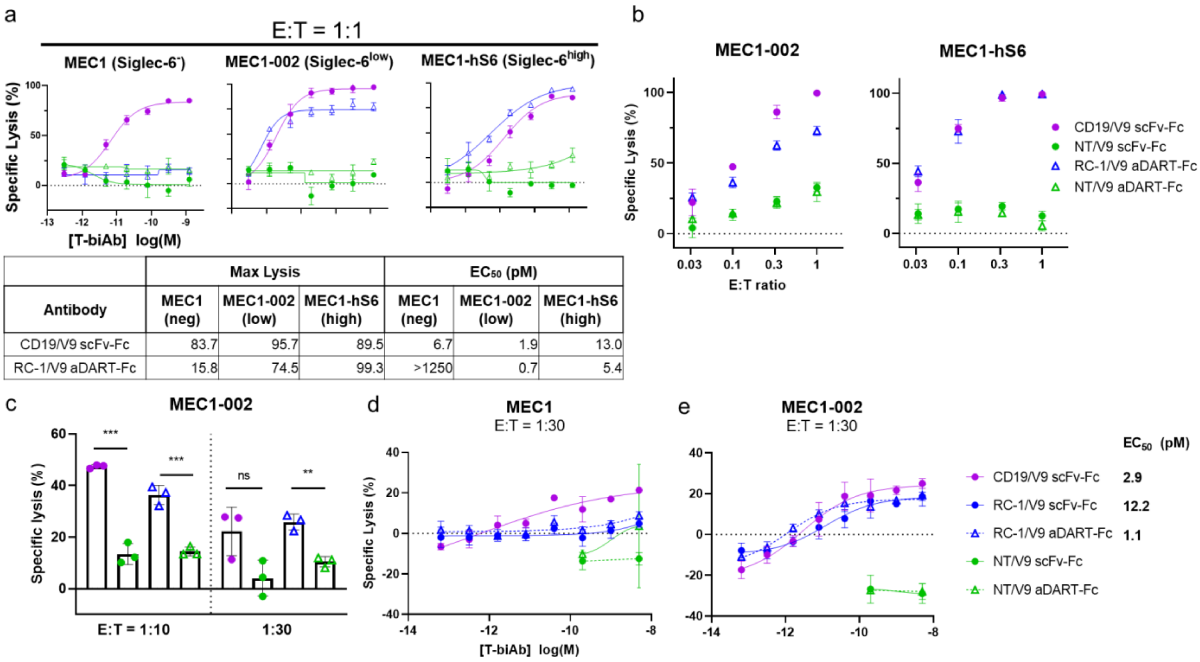

Antibody	Max Lysis			EC_{50} (pM)		
	MEC1 (neg)	MEC1-002 (low)	MEC1-hS6 (high)	MEC1 (neg)	MEC1-002 (low)	MEC1-hS6 (high)
CD19/V9 scFv-Fc	83.7	95.7	89.5	6.7	1.9	13.0
RC-1/V9 aDART-Fc	15.8	74.5	99.3	>1250	0.7	5.4

Figure S8: RC-1/V9 aDART-Fc efficacy on low expression MEC1-002 cells and at low E:T ratios. (a) Cytotoxicity of an overnight co-culture at a 1:1 E:T ratio with Siglec-6-negative (MEC1), -low (MEC1-002), or -high (MEC1-hS6) expression cell lines, in the presence of titrated T-biAb. (b, c) Cytotoxicity assays consisting of a 48 h co-culture of 1 nM T-biAb, 50,000 MEC1-002 or MEC1-hS6 target cells, and a titration of T cells from 50,000 down to 1,500 cells/sample. (c) Bar graph comparing specific lysis at 1:10 and 1:30 E:T ratios for CD19/V9 scFv-Fc or RC-1/V9 aDART-Fc demonstrating that specific lysis is still achieved at 1:30 E:T ratio even with relatively low Siglec-6 expression on MEC1-002 cells. Siglec-6 targeting scFv-Fc and aDART-Fc were titrated against target-negative (MEC1, d) or target-low (MEC1-002, e) cells with a 1:30 E:T ratio of T cells over a 48 h co-culture and the EC_{50} values for RC-1/V9 aDART-Fc were more than 10-fold lower than that of the RC-1/V9 scFv-Fc and almost 3-fold lower than the CD19/V9 scFv-Fc.

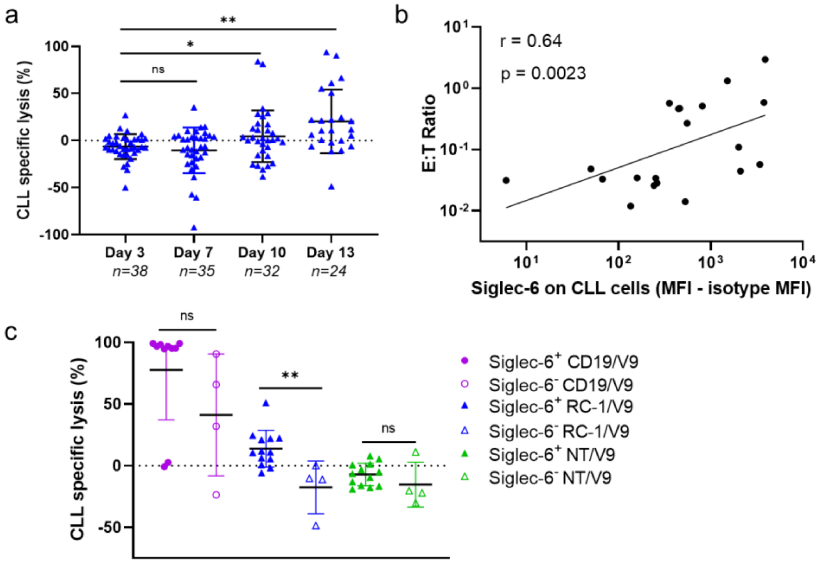

Figure S9: Targeting Siglec-6 on primary CLL cells. (a) CLL PBMC were co-cultured with RC-1/V9 aDART-Fc (6 nM) for 3 to 13 days and analyzed by flow cytometry to determine specific lysis of CLL cells. Statistics were calculated to compare different time points using a Wilcoxon matched-pairs signed rank test. (b) Siglec-6 expression and E:T ratio were established at baseline and these variables correlated by Spearman's correlation analysis. (c) Specific lysis data from day 13, separating patients based on Siglec-6 expression. Statistics were calculated using the Mann-Whitney test.

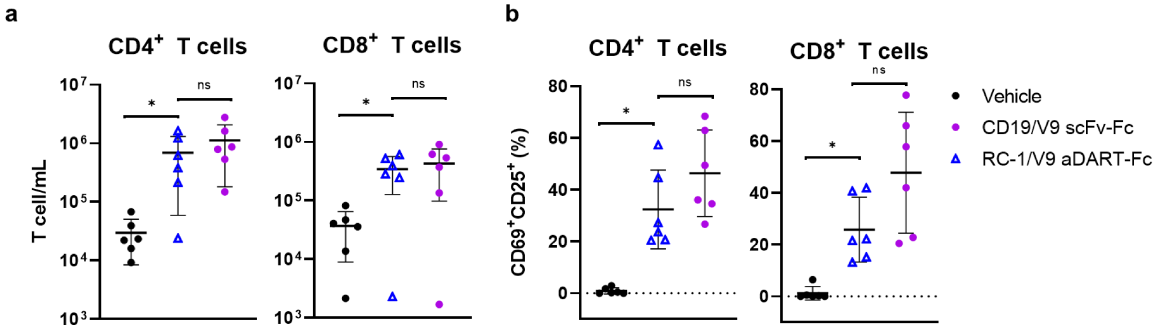

Figure S10: CLL-derived T cell expansion and activation. (a) CLL PBMC were cultured with RC-1/V9 aDART-Fc or CD19/V9 scFv-Fc (6 nM) for 9 days and analyzed by flow cytometry to quantify the number of CD4+ and CD8+ T cells present. (b) Also at day 9, the fraction of each subset expressing both CD25 and CD69 activation markers was quantified. Statistics were calculated using the Wilcoxon matched-pairs signed rank test.

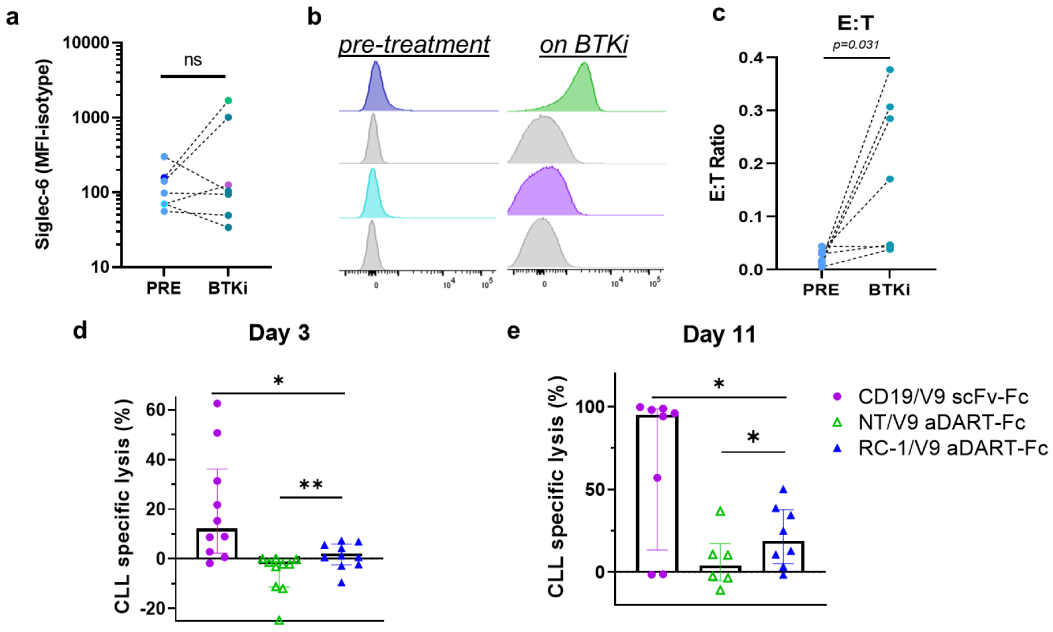

Figure S11: Siglec-6 in BTKi-treated CLL patients. Siglec-6 expression (a-b) for CLL patients before and after beginning BTKi therapy (n=7). (c) E:T ratio for CLL patients before and after beginning BTKi therapy. Samples from these BTKi-treated patients were also tested for cytotoxicity elicited by 6 nM T-biAb in *ex vivo* cultures at day 3 (d, n=10) and day 11 (e, n=8). Please note that BTKi treatment pressure was not applied during *ex vivo* culture. All paired statistics are based on Wilcoxon analyses.

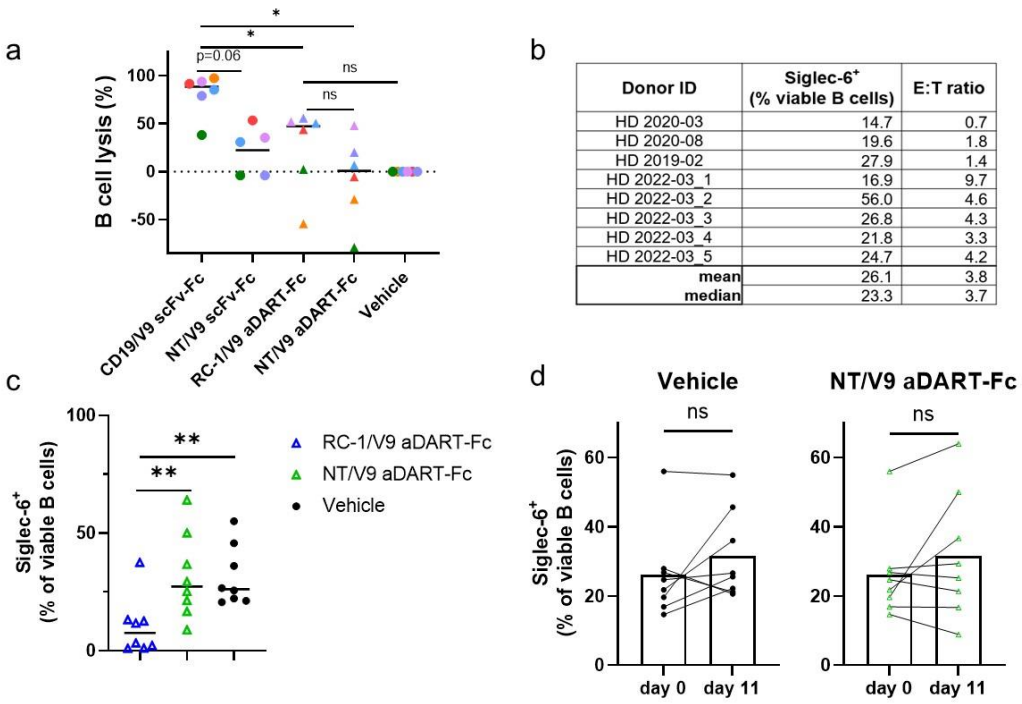

Donor ID	Siglec-6$^+$ (% viable B cells)	E:T ratio
HD 2020-03	14.7	0.7
HD 2020-08	19.6	1.8
HD 2019-02	27.9	1.4
HD 2022-03_1	16.9	9.7
HD 2022-03_2	56.0	4.6
HD 2022-03_3	26.8	4.3
HD 2022-03_4	21.8	3.3
HD 2022-03_5	24.7	4.2
mean	26.1	3.8
median	23.3	3.7

Figure S12: Siglec-6 T-biAb treatment of healthy donor PBMC. (a) Healthy donor PBMC (n=6; n=5 for NT/V9 scFv-Fc) were cultured with T-biAbs, using conditions identical to the CLL lysis assays, and specific healthy B cell lysis = (Viability$_{vehicle}$ - Viability$_{treated}$) / Viability$_{vehicle}$ was assessed on day 11. Statistics were calculated using the Wilcoxon test. Color coding corresponds to paired samples from individual healthy donors. (b) Siglec-6 expression and T cell to B cell (E:T) ratios in for healthy donor (HD) PBMC. (c) The fraction of viable healthy B cells expressing Siglec-6 after 11-day *ex vivo* culture in the presence or absence of T-biAbs. (Note: CD19/V9 data are not shown, as too few viable B cells were remaining to conduct reliable statistical analyses). Statistics were calculated using the Wilcoxon test (n=8). (d) The fraction of healthy B cells expressing Siglec-6 at baseline (day 0) and day 11. Statistics were calculated using the Wilcoxon test (n=8).

SUPPLEMENTAL TABLES

Table S1: HDX-MS experimental conditions and data analysis parameters from the guidelines of the IC-HDX-MS community.

Data Set (Figures 1 and S3)	Siglec-6 +/- RC-1 Fab
HDX reaction details	10 mM Sodium phosphate, 150 mM NaCl, pH = 7.4, 4 °C
HDX quench reaction details	3 M Urea, 1% TFA, pH = 2.5, 4 °C
HDX time course (seconds)	10, 30, 60, 300, 900, and 3600
Back-exchange	estimated from input recovery estimate of 0.7 and deuterium solution concentration of 0.8
# of Peptides	28
Sequence coverage	55 %
Average peptide length / Redundancy	10 / 3.653
Replicates (biological or technical)	3 technical replicates
Repeatability	3.120461 (average STD)
Significant differences in HDX	> 5 %D (unpaired t-tests at each time point, p-value < 0.01)

HDX = hydrogen deuterium exchange, TFA = trifluoroacetic acid, %D = percent deuterium

Table S2: CLL patient characteristics

Patient ID	Siglec-6 MFI	E :T	Age/ Gender	Rai Stage	Treatment History	IGHV Status (mutated/ unmutated)	Cytogenetics	ALC ($x10^3$/µL)
2691	161.0	1:15.2	58/M	2	TN	U	N/A	113.52
3071	147.0	1:14.5	67/M	4	TN	M	trisomy 12	131.32
11944	96.8	1:47.6	53/M	2	TN	U	trisomy 12	278.35
4086	69.4	1:35.7	53/M	2	TN	U	N/A	94.86
4973	66.6	1:27.0	50/M	4	TN	M	del13q,del17p	68.97
8242	64.3	1:58.8	81/F	1	TN	M	del13q	202.06
4705	61.4	1:33.3	58/M	1	TN	M	N/A	49.5
4653	59.6	1:71.4	46/M	1	TN	M	del13q	153.59
2356	59.4	1:8.7	31/M	4	TN	M	del13q,del11q	4.7
4296	42.8	1:27.8	74/F	2	RR	N/A	N/A	142.3
2501	42.4	1:200.0	N/A/F	N/A	TN	N/A	N/A	N/A
10515	41.5	1:37.0	66/F	1	TN	M	del13q	123.11
5403	38.9	1:500.0	65/F	3	RR	N/A	del13q,del17p	238.86
11682	33.7	1:15.6	55/F	1	TN	U	Normal	150.38
5022	32.0	1:100.0	48/M	3	TN	U	del13q,del17p	557.64
5918	25.8	1:27.8	65/F	1	TN	M	del13q	53.45

Available information for the n=16 CLL patients initially assessed for Siglec-6-targeting therapy. MFI= mean fluorescence intensity; E:T = effector to target ratio; TN = treatment naïve; RR = relapsed/refractory; IGHV= immunoglobulin heavy chain status: M = mutated, U = unmutated; ALC = absolute lymphocyte count; N/A = not available.

Table S3: Representative viability and cell count data from CLL cytotoxicity assays

Day 11 treatment-naïve CLL cell lysis					
patient	**treatment**	**Single cell viable (#)**	**Single cell viable (% of single cell)**	**CLL cell viable (#)**	**CLL cell viable (% of CLL cell)**
2501	CD19/V9 scFv-Fc	4102	48.7	1944	34.1
2501	RC-1/V9 scFv-Fc	8756	55.2	5508	46.4
2501	JML-1/V9 scFv-Fc	12753	56.7	9067	51.0
2501	NT/V9 scFv-Fc	9451	59.2	7712	56.2
2501	RC-1/V9 aDART-Fc	12104	51.8	7759	43.7
2501	NT/V9 aDART-Fc	11663	58.2	10135	56.0
2501	None	16584	59.9	15009	58.2
4973	CD19/V9 scFv-Fc	5197	36.8	28	6.4
4973	RC-1/V9 scFv-Fc	6857	65.0	1241	57.0
4973	JML-1/V9 scFv-Fc	4751	55.0	51	28.3
4973	NT/V9 scFv-Fc	10089	63.3	423	36.8
4973	RC-1/V9 aDART-Fc	9706	57.4	55	27.4
4973	NT/V9 aDART-Fc	6656	57.5	272	41.4
4973	None	3802	56.6	605	47.1
8242	CD19/V9 scFv-Fc	1675	27.4	70	6.0
8242	RC-1/V9 scFv-Fc	14285	70.2	1743	45.0
8242	JML-1/V9 scFv-Fc	18631	72.3	1852	48.2
8242	NT/V9 scFv-Fc	10476	74.3	2849	59.5
8242	RC-1/V9 aDART-Fc	12131	60.1	986	32.3
8242	NT/V9 aDART-Fc	5516	65.8	1594	59.1
8242	None	5896	64.0	1680	46.1
11944	CD19/V9 scFv-Fc	11292	51.6	338	6.6
11944	RC-1/V9 scFv-Fc	12992	65.1	1871	28.8
11944	JML-1/V9 scFv-Fc	6615	30.3	1740	13.2
11944	NT/V9 scFv-Fc	11591	73.4	4857	58.1
11944	RC-1/V9 aDART-Fc	10855	51.4	403	6.8
11944	NT/V9 aDART-Fc	5968	54.1	3127	41.6
11944	None	3804	40.9	2305	33.8
4296	CD19/V9 scFv-Fc	5636	42.0	3985	42.2
4296	RC-1/V9 scFv-Fc	7458	54.2	5638	55.2
4296	JML-1/V9 scFv-Fc	7208	51.3	5089	50.4
4296	NT/V9 scFv-Fc	3831	60.1	2180	55.0
4296	RC-1/V9 aDART-Fc	2673	59.3	1617	56.5
4296	NT/V9 aDART-Fc	10956	68.9	5971	61.0
4296	None	6922	52.8	5780	52.7
10515	CD19/V9 scFv-Fc	1490	50.4	565	39.4
10515	RC-1/V9 scFv-Fc	8772	67.9	4465	62.6
10515	JML-1/V9 scFv-Fc	9628	72.7	4968	68.5
10515	NT/V9 scFv-Fc	2253	59.2	820	45.2
10515	RC-1/V9 aDART-Fc	9900	75.0	5950	73.8
10515	NT/V9 aDART-Fc	10557	75.8	5342	68.6
10515	None	7225	71.1	5823	71.2
11682	CD19/V9 scFv-Fc	2616	24.6	874	11.9
11682	RC-1/V9 scFv-Fc	3950	54.0	1232	36.1
11682	JML-1/V9 scFv-Fc	6284	51.3	2218	35.9
11682	NT/V9 scFv-Fc	10383	72.4	2689	50.1
11682	RC-1/V9 aDART-Fc	5304	70.7	1416	49.4
11682	NT/V9 aDART-Fc	10301	69.6	3111	45.1
11682	None	3152	41.5	1800	31.1

Day 13 treatment-naïve CLL cell lysis				
Sample:	**Single cell viable (#)**	**Single cell viable (% of single cell)**	**CLL cell viable (#)**	**CLL cell viable (% of CLL cell)**
11192_Siglec_E04_021.fcs	65442	58.4	25987	54.0
11192_NT_E03_020.fcs	66160	53.4	29594	59.6
11192_untreated_E01_018.fcs	56497	47.5	28151	60.4
11192_19,2f,3_E02_019.fcs	19888	17.7	650	1.9
11627_Siglec_C04_013.fcs	12931	47.3	2870	52.4
11627_NT_C03_012.fcs	21713	61.0	3466	56.0
11627_Untreated_C01_011.fcs	35557	57.4	4222	49.5
12033_Siglec_D04_017.fcs	63143	21.2	10338	54.3
12033_NT_D03_016.fcs	82674	50.0	22783	81.8
12033_Untreated_D01_014.fcs	65428	26.1	13259	68.7
12033_19,2f,3_D02_015.fcs	40119	17.4	277	3.6
12202_Siglec_B04_010.fcs	65259	44.5	20886	70.4
12202_NT_B03_009.fcs	56062	69.3	28389	86.7
12202_Untreated_B01_007.fcs	53714	54.8	40240	79.1
12202_19,2f,3_B02_008.fcs	52339	36.6	62	0.7
5539 PBMC_Siglec_E01_010.fcs	78041	50.2	15746	39.4
5539 PBMC_NT_D01_009.fcs	49424	70.0	28901	74.1
5539 PBMC_Untreated_B01_007.fcs	32209	77.9	23699	80.4
5539 PBMC_19,2f,3_C01_008.fcs	125207	60.1	767	4.0
8289 PBMC_Siglec_E02_014.fcs	62913	54.1	19153	66.6
8289 PBMC_NT_D02_013.fcs	45972	68.6	35554	82.9
8289 PBMC_Untreated_B02_011.fcs	16263	68.5	9865	71.1
8289 PBMC_19,2f,3_C02_012.fcs	45523	42.2	203	2.2
11597 PBMC_Siglec_E03_018.fcs	69413	56.9	42424	71.9
11597 PBMC_NT_D03_017.fcs	15174	43.2	13064	43.0
11597 PBMC_Untreated_B03_015.fcs	18678	48.4	16717	48.4
11597 PBMC_19,2f,3_C03_016.fcs	65924	62.2	30858	59.8
4086 PBMC_Siglec_E03_017.fcs	4413	6.4	3029	6.4
4086 PBMC_NT_D03_016.fcs	182665	78.0	160656	83.4
4086 PBMC_Untreated_B03_014.fcs	171000	65.5	133048	68.4
4086 PBMC_19,2f,3_C03_015.fcs	203183	72.2	143426	76.1
5407 PBMC_Siglec_E02_013.fcs	198408	58.0	174709	63.2
5407 PBMC_NT_D02_012.fcs	366499	80.3	341752	82.4
5407 PBMC_Untreated_B02_010.fcs	296113	62.6	265734	63.3
5407 PBMC_19,2f,3_C02_011.fcs	218573	47.4	131963	43.1
5508 PBMC_Siglec_E01_009.fcs	137437	61.3	76848	63.4
5508 PBMC_NT_D01_008.fcs	317754	79.9	210636	85.7
5508 PBMC_Untreated_B01_007.fcs	228296	78.7	164775	81.6

Day 7 treatment-naïve CLL cells + allogeneic T cells				
Sample:	**Single cell viable (#)**	**Single cell viable (% of single cell)**	**CLL cell viable (#)**	**CLL cell viable (% of CLL cell)**
DAY7 Siglec Mix 5539_UT_B04_019.fcs	105579	64.1	25861	55.2
DAY7 Siglec Mix 5539_19_3_C04_020.fcs	1541	1.1	739	1.7
DAY7 Siglec Mix 5539_NT_D04_021.fcs	78467	58.9	26836	62.8
DAY7 Siglec Mix 5539_SIG_E04_022.fcs	126773	61.0	20017	46.8
DAY7 Siglec Mix 8289_UT_B05_023.fcs	145145	74.5	68998	86.9
DAY7 Siglec Mix 8289_19_3_C05_024.fcs	99437	49.5	3163	11.3
DAY7 Siglec Mix 8289_NT_D05_025.fcs	73532	67.7	29722	82.6

DAY7 Siglec Mix 8289_SIG_E05_026.fcs	135502	67.7	37906	69.4
DAY7 Siglec Mix 11597_UT_B06_027.fcs	141951	75.2	60816	82.6
DAY7 Siglec Mix 11597_19_3_C06_028.fcs	78866	40.4	1326	3.5
DAY7 Siglec Mix 11597_NT_D06_029.fcs	97317	63.8	59682	85.4
DAY7 Siglec Mix 11597_SIG_E06_030.fcs	187476	71.5	65263	82.4
4086 Mix_Siglec_E06_029.fcs	130752	62.5	52314	64.3
4086 Mix_NT_D06_028.fcs	41004	39.6	20051	46.7
4086 Mix_Untreated_B06_026.fcs	43522	63.8	17685	65.4
4086 Mix_19,2f,3_C06_027.fcs	97715	50.4	2554	7.0
5407 Mix_Siglec_E04_021.fcs	158203	76.8	89572	79.5
5407 Mix_NT_D04_020.fcs	138000	72.7	106356	85.8
5407 Mix_Untreated_B04_018.fcs	240469	85.0	163361	87.7
5407 Mix_19,2f,3_C04_019.fcs	168877	62.4	84880	59.2
5508 Mix_Siglec_E05_025.fcs	50729	55.5	5941	31.7
5508 Mix_NT_D05_024.fcs	57524	73.6	33394	85.4
5508 Mix_Untreated_B05_022.fcs	139944	88.4	59214	92.8
5508 Mix_19,2f,3_C05_023.fcs	111327	53.3	7508	16.6

Table S4: BTKi-treated CLL patient characteristics

Sample ID	% Siglec-6+ (live CLL cells)	Siglec-6 MFI	E : T		BTKi	Timepoint	Age/Gender	Treatment history	Rai Stage	IGHV Status	Cytogenetics	ALC, k/µ
9746	4	141.8	1:	55.1	PRE	0	64/M	TN	3	U	del13q	93.4
12032	67.6	1943	1:	3.1	acalabrutinib	28	67/M	TN	3	U	del13q, NOTCH1	3.6
8330	1.69	157.2	1:	90.5	PRE	0	53/F	RR	3	M	del13q	178.1
11913	95.5	3154	1:	4.0	acalabrutinib	48	57/F	RR	3	M	del13q	7.6
9132	0.38	55.6	1:	22.5	PRE	0	65/M	RR	4	U	del11q, del14q	120
9778	2.26	49	1:	23.3	acalabrutinib	6	65/M	RR	4	U	del11q, del14q	129.8
9450	0.62	69.9	1:	199.0	PRE	0	68/F	TN	3	U	del13q, del17p	225.8
9939	8.18	125.7	1:	26.0	acalabrutinib	6	68/F	TN	3	U	del13q, del17p	36.6
6811	1.57	98	1:	33.7	PRE	0	70/M	TN	4	M	del13q, del17p	86.3
7791	13.5	93.9	1:	21.2	ibrutinib	6	71/M	TN	4	M	del13q, del17p	65.8
7786	2.87	300.7	1:	64.3	PRE	0	66/M	TN	1	ND	del13q, Tri12	257.5
9153	18.4	104	1:	3.3	ibrutinib	24	68/M	TN	1	ND	del13q, Tri12	5.3
7562	0.68	70.6	1:	28.4	PRE	0	66/F	RR	4	U	del11q, del13q	155.5
8156	3.87	34	1:	5.8	ibrutinib	12	67/F	RR	4	U	del11q, del13q	6.71

Timepoint = time since starting treatment; MFI= mean fluorescence intensity; IGHV= immunoglobulin heavy chain; status: m=mutated, u=unmutated; ALC= absolute lymphocyte count.

Table S5: Healthy donor B cell viability

	CD19/V9 scFv-Fc	NT/V9 scFv-Fc	RC-1/V9 aDART-Fc	NT/V9 aDART-Fc	Vehicle
1	~~10.9~~	~~11.6~~	~~21.1~~	~~28.3~~	~~18.6~~
2	~~3.2~~	~~8.3~~	~~11.4~~	~~17.0~~	~~19.3~~
3	3.2	17.8	21.4	40.2	38.2
4	1.0		51.3	42.9	33.3
5	~~4.3~~	~~18.1~~	~~17.5~~	~~19.5~~	~~7.2~~
6	12.8	21.5	20.2	37.0	20.7
7	6.8	31.8	22.8	42.9	46.1
8	6.9	33.6	14.3	25.8	32.4
9	2.3	23.0	17.1	18.5	35.7

Healthy donor B cells were cultured identically to the CLL patient samples with the indicated T-biAbs or vehicle control (DPBS). Overall, B cell survival *ex vivo* was variable. Out of the samples tested (n = 9), three of the healthy donors were excluded from analysis (red, strikethrough) as the vehicle control viability was below the 20% threshold value. These data were used to calculate specific lysis values presented in Figure S12.

Table S6. Pharmacokinetic parameters of RC-1/V9 aDART-Fc

Route	Conditioning	Half-life (h)	AUC (mg x h x mL^{-1})	CL (mL x h^{-1} x kg^{-1})	V_{ss} (mL x kg^{-1})
IV	-	170 ± 67	4.9 ± 0.5	0.51 ± 0.06	120 ± 40
IV	human serum	190 ± 17	4.8 ± 0.4	0.53 ± 0.05	117 ± 18
IP	-	254 ±114	6.8 ± 2.3	0.40 ± 0.14	
IP	human serum	218 ± 59	6.2 ± 1.4	0.42 ± 0.10	

NSG mice were preconditioned with 250 µL of human serum by intraperitoneal (i.p.) injection 24 h prior to injection of 50 µg (2.5 mg/kg) RC-1/V9 aDART-Fc by i.v. or i.p. injection. Blood was collected from the tail vein at various time points over the course of 22 days, and T-biAbs in the serum were detected by ELISA, which consisted of capturing recombinant CD3ε/δ dimer and detecting with an anti-human Fc secondary. The values in the table are the averages and standard deviations for 3 (i.v. +serum cage) to 4 (all others) mice per treatment group. AUC = area under curve. CL = clearance. Vss = steady state volume of distribution.

AMINO ACID SEQUENCES

RC-1 clone V_H
EVQLVESGGGLVQPGRSLRLSCAASGFTFSSYGMHWVRQAPGKGLEWVAVISYDGSNKYYA
DSVKGRFTISRDNSKNTLYLQMNSLRAEDTAVYYCANYGMDVWGKGTTVTVSS

RC-1 clone $V_κ$
AIRLTQSPSSLSASVGDRVTITCRASQSISSYLNWYQQKPGKAPKLLIYAASSLQSGVPSRFSG
SGSGTDFTLTISSLQPEDFATYYCQQSYGTPFTFGPGTKVDIK

RC-2 clone V_H
EVQLLESGGGVVQPGRSLRLSCAASGFTFSSYGMHWVRQAPGKGLEWVAVISYDGSNKHYA
DSVKGRFTISRDNSKNTLYLQMNSLRAEDTAVYYCARGGQTIDIWGQGTMVTVSS

RC-2 clone $V_κ$
DIVMTQSPSSLSASVGDRVTITCRASQSISSYLNWYQQKPGKAPKLLIYAASSLQSGVPSRFSG
SGSGTDFTLTISSLQPEDFATYYCQQSYSTPYTFGQGTKLEIK

Sequence of Siglec-6 VC_{28-235}-His6 in pHL-sec
etgERRFQLEGPESLTVQEGLCVLVPCRLPTTLPASYYGYGYWFLEGADVPVATNDPDEEVQE
ETRGRFHLLWDPRRKNCSLSIRDARRRDNAAYFFRLKSKWMKYGYTSSKLSVRVMALTHRPNI
SIPGTLESGHPSNLTCSVPWVCEQGTPPIFSWMSAAPTSLGPRTTQSSVLTITPRPQDHSTNLT
CQVTFPGAGVTMERTIQLNVSgtkhhhhhh

Sequence of JML-1 scFv-Fc with aglycosylation N297A and "knob" mutations (S354C, T366W)
KVQLLESGGGLVQPGRSLRLSCAASGFTFDDYGMHWVRQAPGKGLEWVSGISWNSGSIGYA
DSVKGRFTISRDNSKNTLYLQMNSLRAEDTAVYYCARGGQTIDIWGQGTMVTVSSGGGGSGG
GGSGGGGSDIQMTQSPSSLSASVGDRVTITCRASQSISSYLNWYQQKPGKAPKLLIYAASSLQ
SGVPSRFSGSGSGTDFTLTISSLQPEDFATYYCQQSYSTPFTFGPGTKVDIKEPKSSDKTHTCP
PCPAPELLGGPSVFLFPPKPKDTLMISRTPEVTCVVVDVSHEDPEVKFNWYVDGVEVHNAKTK
PREEQYASTYRVVSVLTVLHQDWLNGKEYKCKVSNKALPAPIEKTISKAKGQPREPQVYTLPP
CRDELTKNQVSLWCLVKGFYPSDIAVEWESNGQPENNYKTTPPVLDSDGSFFLYSKLTVDKSR
WQQGNVFSCSVMHEALHNHYTQKSLSLSPGA

Sequence of RC-1 scFv-Fc with aglycosylation N297A and "knob" mutations (S354C, T366W)
EVQLVESGGGLVQPGRSLRLSCAASGFTFSSYGMHWVRQAPGKGLEWVAVISYDGSNKYYA
DSVKGRFTISRDNSKNTLYLQMNSLRAEDTAVYYCANYGMDVWGKGTTVTVSSGGGGSGGG
GSGGGGSAIRLTQSPSSLSASVGDRVTITCRASQSISSYLNWYQQKPGKAPKLLIYAASSLQSG
VPSRFSGSGSGTDFTLTISSLQPEDFATYYCQQSYGTPFTFGPGTKVDIKEPKSSDKTHTCPPC
PAPELLGGPSVFLFPPKPKDTLMISRTPEVTCVVVDVSHEDPEVKFNWYVDGVEVHNAKTKPR
EEQYASTYRVVSVLTVLHQDWLNGKEYKCKVSNKALPAPIEKTISKAKGQPREPQVYTLPPCR
DELTKNQVSLWCLVKGFYPSDIAVEWESNGQPENNYKTTPPVLDSDGSFFLYSKLTVDKSRW
QQGNVFSCSVMHEALHNHYTQKSLSLSPGA

Sequence of shared anti-CD3 (V9 clone) with Fc with aglycosylation N297A and "hole" mutations (Y349C, T366S, L368A, and Y407)
EVQLVESGGGLVQPGGSLRLSCAASGYSFTGYTMNWVRQAPGKGLEWVALINPYKGVSTYN
QKFKDRFTISVDKSKNTAYLQMNSLRAEDTAVYYCARSGYYGDSDWYFDVWGQGTLVTVSSG
GGGSGGGGSGGGGSDIQMTQSPSSLSASVGDRVTITCRASQDIRNYLNWYQQKPGKAPKLLI

YYTSRLESGVPSRFSGSGSGTDYTLTISSLQPEDFATYYCQQGNTLPWTFGQGTKVEIKEPKS
SDKTHTCPPCPAPELLGGPSVFLFPPKPKDTLMISRTPEVTCVVVDVSHEDPEVKFNWYVDGV
EVHNAKTKPREEQYASTYRVVSVLTVLHQDWLNGKEYKCKVSNKALPAPIEKTISKAKGQPRE
PQVCTLPPSRDELTKNQVSLSCAVKGFYPSDIAVEWESNGQPENNYKTTPPVLDSDGSFFLVS
KLTVDKSRWQQGNVFSCSVMHEALHNHYTQKSLSLSPGA

Sequence of V9/RC-1 sDART-Fc

Chain 1:

DIQMTQSPSSLSASVGDRVTITCRASQDIRNYLNWYQQKPGKAPKLLIYYTSRLESGVPSRFSG
SGSGTDYTLTISSLQPEDFATYYCQQGNTLPWTFGQGTKVEIKGGGSGGGGEVQLVESGGGL
VQPGRSLRLSCAASGFTFSSYGMHWVRQAPGKGLEWVAVISYDGSNKYYADSVKGRFTISRD
NSKNTLYLQMNSLRAEDTAVYYCANYGMDVWGKGTTVTVSSGCPPCPAPEAAGGPSVFLFPP
KPKDTLMISRTPEVTCVVVDVSHEDPEVKFNWYVDGVEVHNAKTKPREEQYNSTYRVVSVLTV
LHQDWLNGKEYKCKVSNKALGAPIEKTISKAKGQPREPQVCTLPPSRDELTKNQVSLSCAVKG
FYPSDIAVEWESNGQPENNYKTTPPVLDSDGSFFLVSKLTVDKSRWQQGNVFSCSVMHEALH
NRFTQKSLSLSPGA

Chain 2:

AIRLTQSPSSLSASVGDRVTITCRASQSISSYLNWYQQKPGKAPKLLIYAASSLQSGVPSRFSG
SGSGTDFTLTISSLQPEDFATYYCQQSYGTPFTFGPGTKVDIKGGGGSGGGGEVQLVESGGG
LVQPGGSLRLSCAASGYSFTGYTMNWVRQAPGKGLEWVALINPYKGVSTYNQKFKDRFTISV
DKSKNTAYLQMNSLRAEDTAVYYCARSGYYGDSDWYFDVWGQGTLVTVSSGCPPCPAPEAA
GGPSVFLFPPKPKDTLMISRTPEVTCVVVDVSHEDPEVKFNWYVDGVEVHNAKTKPREEQYN
STYRVVSVLTVLHQDWLNGKEYKCKVSNKALGAPIEKTISKAKGQPREPQVYTLPPCRDELTKN
QVSLWCLVKGFYPSDIAVEWESNGQPENNYKTTPPVLDSDGSFFLYSKLTVDKSRWQQGNVF
SCSVMHEALHNHYTQKSLSLSPGA

Sequence of RC-1/V9 sDART-Fc

Chain 1:

AIRLTQSPSSLSASVGDRVTITCRASQSISSYLNWYQQKPGKAPKLLIYAASSLQSGVPSRFSG
SGSGTDFTLTISSLQPEDFATYYCQQSYGTPFTFGPGTKVDIKGGGSGGGGEVQLVESGGGLV
QPGGSLRLSCAASGYSFTGYTMNWVRQAPGKGLEWVALINPYKGVSTYNQKFKDRFTISVDK
SKNTAYLQMNSLRAEDTAVYYCARSGYYGDSDWYFDVWGQGTLVTVSSGCPPCPAPEAAGG
PSVFLFPPKPKDTLMISRTPEVTCVVVDVSHEDPEVKFNWYVDGVEVHNAKTKPREEQYNSTY
RVVSVLTVLHQDWLNGKEYKCKVSNKALGAPIEKTISKAKGQPREPQVCTLPPSRDELTKNQV
SLSCAVKGFYPSDIAVEWESNGQPENNYKTTPPVFDSDGSFFLVSKLTVDKSRWQQGNVFSC
SVMHEALHNRFTQKSLSLSPGA

Chain 2:

DIQMTQSPSSLSASVGDRVTITCRASQDIRNYLNWYQQKPGKAPKLLIYYTSRLESGVPSRFSG
SGSGTDYTLTISSLQPEDFATYYCQQGNTLPWTFGQGTKVEIKGGGGSGGGGEVQLVESGGG
LVQPGRSLRLSCAASGFTFSSYGMHWVRQAPGKGLEWVAVISYDGSNKYYADSVKGRFTISR
DNSKNTLYLQMNSLRAEDTAVYYCANYGMDVWGKGTTVTVSSGCPPCPAPEAAGGPSVFLFP
PKPKDTLMISRTPEVTCVVVDVSHEDPEVKFNWYVDGVEVHNAKTKPRVSLWCLVKGFYPSDI
AVEWESNGQPENNYKTTPPVLDSDGSFFLYSKLTVDKSRWQQGNVFSCSVMHEALHNHYTQ
KSLSLSPGA

Sequence of RC-1/V9 aDART-Fc

Chain 1:

AIRLTQSPSSLSASVGDRVTITCRASQSISSYLNWYQQKPGKAPKLLIYAASSLQSGVPSRFSG
SGSGTDFTLTISSLQPEDFATYYCQQSYGTPFTFGPGTKVDIKGGGSGGGGEVQLVESGGGLV
QPGGSLRLSCAASGYSFTGYTMNWVRQAPGKGLEWVALINPYKGVSTYNQKFKDRFTISVDK
SKNTAYLQMNSLRAEDTAVYYCARSGYYGDSDWYFDVWGQGTLVTVSSASTKGEVAACEKE

VAALEKEVAALEKEVAALEKGGGDKTHTCPPCPAPEAAGGPSVFLFPPKPKDTLMISRTPEVTC
VVVDVSHEDPEVKFNWYVDGVEVHNAKTKPREEQYNSTYRVVSVLTVLHQDWLNGKEYKCK
VSNKALGAPIEKTISKAKGQPREPQVYTLPPCRDELTKNQVSLWCLVKGFYPSDIAVEWESNG
QPENNYKTTPPVLDSDGSFFLYSKLTVDKSRWQQGNVFSCSVMHEALHNHYTQKSLSLSPGA
Chain 2:
DIQMTQSPSSLSASVGDRVTITCRASQDIRNYLNWYQQKPGKAPKLLIYYTSRLESGVPSRFSG
SGSGTDYTLTISSLQPEDFATYYCQQGNTLPWTFGQGTKVEIKGGGGSGGGGEVQLVESGGG
LVQPGRSLRLSCAASGFTFSSYGMHWVRQAPGKGLEWVAVISYDGSNKYYADSVKGRFTISR
DNSKNTLYLQMNSLRAEDTAVYYCANYGMDVWGKGTTVTVSSASTKGKVAACKEKVAALKEK
VAALKEKVAALKE
Chain 3:
DKTHTCPPCPAPEAAGGPSVFLFPPKPKDTLMISRTPEVTCVVVDVSHEDPEVKFNWYVDGVE
VHNAKTKPREEQYNSTYRVVSVLTVLHQDWLNGKEYKCKVSNKALGAPIEKTISKAKGQPREP
QVCTLPPSRDELTKNQVSLSCAVKGFYPSDIAVEWESNGQPENNYKTTPPVLDSDGSFFLVSK
LTVDKSRWQQGNVFSCSVMHEALHNRFTQKSLSLSPGA